

Brain-metastatic Triple-negative Breast Cancer Cells Regain Growth Ability by Altering Gene Expression Patterns

YOUN KYUNG CHOI^{1*}, SANG-MI WOO^{1*}, SUNG-GOOK CHO^{1*}, HYO EUN MOON^{2,3},
YEE JIN YUN¹, JIN WOOK KIM², DONG-YOUNG NOH⁴, BO HYUNG JANG¹, YONG CHOL SHIN¹,
JEONG-HYUN KIM⁵, HYOUNG DOO SHIN^{5,6}, SUN HA PAEK^{2,3} and SEONG-GYU KO¹

¹Department of Preventive Medicine, College of Korean Medicine, Kyung Hee University, Seoul, Republic of Korea;

²Department of Neurosurgery, ³Cancer Research Institute, Ischemic/Hypoxia Disease Institute and

⁴Department of Surgery, Seoul National University College of Medicine, Seoul, Republic of Korea;

⁵Department of Life Science, Sogang University, Seoul, Korea;

⁶Department of Genetic Epidemiology, SNP Genetics Inc., Seoul, Republic of Korea

Abstract. *Background/Aim:* Triple-negative breast cancer (TNBC) frequently metastasizes to the brain (BrM). However, genes responsible for BrM of TNBC are yet to be identified. *Materials and Methods:* Gene expression profiling of TNBC and BrM was conducted, and studies with cultured cells in vitro were performed to verify functions of genes identified in these analyses. *Results:* According to gene expression analyses of TNBC and BrM, periplakin (PPL) and mitogen-activated protein kinase 13 (MAPK13) were chosen for further investigations. PPL and MAPK13 were highly expressed in TNBC compared to BrM. While silencing of either PPL or MAPK13 in TNBC cells increased cell growth and reduced cell motility, overexpression of either PPL or MAPK13 in BrM cells, retarded growth rates and facilitated cell motility. *Conclusion:* Gene expression patterns in TNBC and BrM reflect cancer cell growth in regions of metastasis.

Biomedical attempts to understand the nature of breast cancer metastases have long been performed (1-8).

*These Authors contributed equally to this work.

Correspondence to: Sun Ha Paek, Department of Neurosurgery, Cancer Research Institute, Ischemic/Hypoxia Disease Institute, Seoul National University College of Medicine, 103 Daehak-ro, Jongno-gu, Seoul, 110-799, South Korea. Tel: +82 220723993, Fax: +82 27448459, e-mail: paeksh@snu.ac.kr and Seong-Gyu Ko, Department of Preventive Medicine, College of Korean Medicine, Kyung Hee University, 1 Hoegi, Seoul, 130-701, South Korea. Tel: +82 29610329, Fax: +82 29661165, e-mail: epiko@khu.ac.kr

Key Words: Triple-negative breast cancer, brain metastasis, PPL, MAPK13.

Intensive efforts have revealed that breast cancer cells frequently metastasize to the lymph nodes, lung, liver, bone, and brain (9), thereby creating need for advances in therapeutic approaches (3, 10-12). However, treatment options for brain metastasis (BrM) of breast cancer are still limited. BrM of breast cancer can be treated by surgery, radiosurgery, and whole-brain radiotherapy (11). In addition, chemotherapeutic approaches can be taken, while the blood-brain barrier is an obstacle to chemotherapy targeting BrM of breast cancer (3, 13).

Breast cancer exists in three molecular subtypes, hormone-positive, human epidermal growth factor receptor 2 (HER2)-positive and triple-negative (2, 7, 8, 14). Triple-negative breast cancer (TNBC) is defined by estrogen receptor-negative, progesterone receptor-negative and HER2-negative expression patterns (2, 9, 14, 15). While TNBC is only identified in approximately 10-15% of patients with breast cancer, it is more aggressive than other subtypes of breast cancer, metastasizes frequently to the brain, and is associated with poor outcomes (9, 10, 15-19). Consequently, BrM of TNBC increases mortality (9, 10, 14, 16-21).

Recent research has investigated genes involved in metastasis of breast cancer (1, 8, 20, 22, 23). However, genes associated with BrM of TNBC are yet to be elucidated. In this study, we analyzed gene expression profiles in TNBC and BrM, and identified several genes significantly up- and down-regulated in BrM compared to TNBC. Expression levels of two genes, periplakin (PPL) and mitogen-activated protein kinase 13 (MAPK13), were uniquely altered in gene expression, ontology and pathway analyses, and were further verified in cultured cells with gain-of-function and loss-of-function approaches. Overall, our investigations demonstrate that TNBC cells lose cell motility but regain growth ability in the brain.

Materials and Methods

Gene expression profiling. Four TNBC and three BrM tissues from patients were used after approval of the Institutional Review Boards in both Seoul National University Hospital (H-0606-021-175) and Kyung Hee University (KHUASP(SE)-12-035). RNAs from either TNBC tissues or BrM tissues from patients were isolated using Trizol reagent. cRNAs were synthesized and hybridized onto Human HT12 genome-wide expression profiling chip (Illumina, San Diego, CA, USA). Data analyses were performed in the GenomeStudio program. Detection of a *p*-value greater than 0.01 was considered meaningful for analyses, an expression level greater than 1 was adjusted to 1, and both fold changes over 5 and delta difference over 50 with a *t*-test *p*-value lower than 0.05 were selected. A heat-map was generated for the expression patterns of significant genes. Hierarchical trees were produced by Pearson correlation. A volcano plot was generated by gene expression levels from the *Z*-scores. Analyses were conducted in Genome Studio software (Illumina) and images were produced in Multiexperimental Viewer (Boston, MA, USA). Gene ontology was analyzed using the gene ontology tree machine. Pathway analysis was conducted based on Kyoto encyclopedia of genes and genomes (KEGG) pathway mapping tool (genome.jp/kegg/pathway.html).

Cell culture. MDA-MB-231 cells, widely used for TNBC studies, were obtained from the American Type Culture Collection (ATCC) (Manassas, VA, USA) and maintained in Dulbecco's Modified Eagle's Medium (DMEM) supplemented with 10% fetal bovine serum and 1% antibiotics. HCC-38, HCC-1395 and HCC-70 cells, defined as TNBC cell lines, were obtained from the Seoul National University Cell Bank (Seoul, Korea) and cultured in Roswell Park Memorial Institute Medium-1640 (RPMI-1640) supplemented with 10% fetal bovine serum and 1% antibiotics. Hs578T cells from Seoul National University Cell Bank were cultured in DMEM. GBL-60 BrM cells were isolated from BrM lesion of TNBC and maintained in DMEM supplemented with 10% fetal bovine serum and 1% antibiotics. For silencing strategies, siRNAs for PPL and MAPK13 were obtained from Santa Cruz BioTech (Santa Cruz, CA, USA). Negative control siRNA (AllStars Negative control) was purchased from Qiagen (Düsseldorf, Germany). For inducing overexpression, BamHI/EcoRI fragment of either full length *PPL* or *MAPK13* was amplified with conventional polymerase chain reaction (PCR) and inserted into pcDNA3.1(+) plasmid (Calsbad, CA, USA). Transient transfections were performed using Lipofectamine mixture with plasmids or siRNAs.

RNA and protein assays. RNAs from patients' tissues and cultured cells were isolated using Trizol (Invitrogen, Calsbad, CA, USA). cDNA was synthesized and subjected to real-time PCR. Primers used were as follows: *PPL*: forward primer: 5'-AGGAGACAGACAG CCTCAGC-3', reverse primer: 5'-GGCTTCTCCTCCATTCTCC-3', *MAPK13*: forward primer: 5'-GGGATGGAGTTCAGTGAGGA-3', reverse primer: 5'-TCACCACGTAGCCAGTCATC-3', Glyceraldehyde 3-phosphate dehydrogenase (*GAPDH*): forward primer: 5'-AATCCCATCACCATTCTCCA-3', reverse primer: 5'-TGGACTC CACGACGTACTCA-3'. Cells were lysed with RIPA buffer, and 30 µg of protein were run on 8% to 12% sodium dodecyl sulfate polyacrylamide gel electrophoresis (SDS-PAGE) and transferred to nitrocellulose membranes. Antibodies for PPL (Abcam, Cat # ab72422, Cambridge, UK) and MAPK13 (Abnova, Cat # PAB2787,

Taipei City, Taiwan) were diluted at 1:500 to 1:1,000. Antibody against actin was obtained from Cell Signaling (Danvers, MA, USA) and used at 1:1,000 dilution.

Cell growth, migration, invasion, anchorage-independent growth assays. Cell numbers were measured for four days, and the doubling time was calculated using the Doubling Time web tool (www.doubling-time.com/compute.php). For cell migration, cells cultured in plates were scratched and cultured for 24 h. Migrated cells were counted after randomly choosing four fields in scratched regions. For invasion assays, two-chamber assays were conducted. Cells were seeded in top chambers pre-coated with matrigel (San Jose, CA, USA) and cultured with 1% serum-enriched medium. The bottom chambers were filled with 10% serum-enriched medium. Twenty four hours after incubation, the top chambers were stained with crystal violet, and invading cells were counted. For anchorage-independent growth assays, cells were cultured in soft agar for 15 days. Colonies were stained with crystal violet and then counted. All experiments were performed in triplicate and repeated three times. The *t*-test was applied to analyze statistical significances. *p*-Values lower than 0.05 were considered statistically significant.

Results

Gene expression patterns between TNBC and BrM. To examine gene expression patterns in TNBC and BrM, gene expression arrays were performed. While gene expression patterns in TNBC were likely to be slightly correlated with those in BrM, expression patterns of several genes were different in TNBC compared to BrM (Figure 1A and B). We further found that approximately 1% out of a total 16,402 genes was significantly differently expressed in TNBC compared to BrM (Table I). In brief, 45 and 74 genes were down-regulated and up-regulated, respectively, in BrM compared to TNBC.

Gene ontology analyses showed that 10 gene ontology categories were altered in BrM compared to TNBC (Table II). Pathway analyses showed that six pathways were most significantly altered in BrM compared to TNBC (Table III). Interestingly, expression of genes associated with cell-to-cell interaction was found to be altered in both pathway and ontology analyses. Overall, mRNA expression levels of *PPL* and *MAPK13* were significantly down-regulated in BrM compared to TNBC, which was also shown in either gene ontology or pathway analyses (Figure 1C).

Expression levels of PPL and MAPK13 in TNBC and BrM. Thus, we further confirmed mRNA expression levels of *PPL* and *MAPK13* in tissues from TNBC and BrM using real-time PCR. Consistent with gene expression array data, mRNA expression levels of *PPL* and *MAPK13* were reduced in BrM compared to TNBC (Figure 2A). Thus, we further examined mRNA expression levels of *PPL* and *MAPK13* in GBL-60 BrM cell line isolated from the brain tumor and TNBC cell lines MDA-MB-231, Hs578T, HCC-70, HCC-38 and HCC-1395. In line with gene expression array data, expression

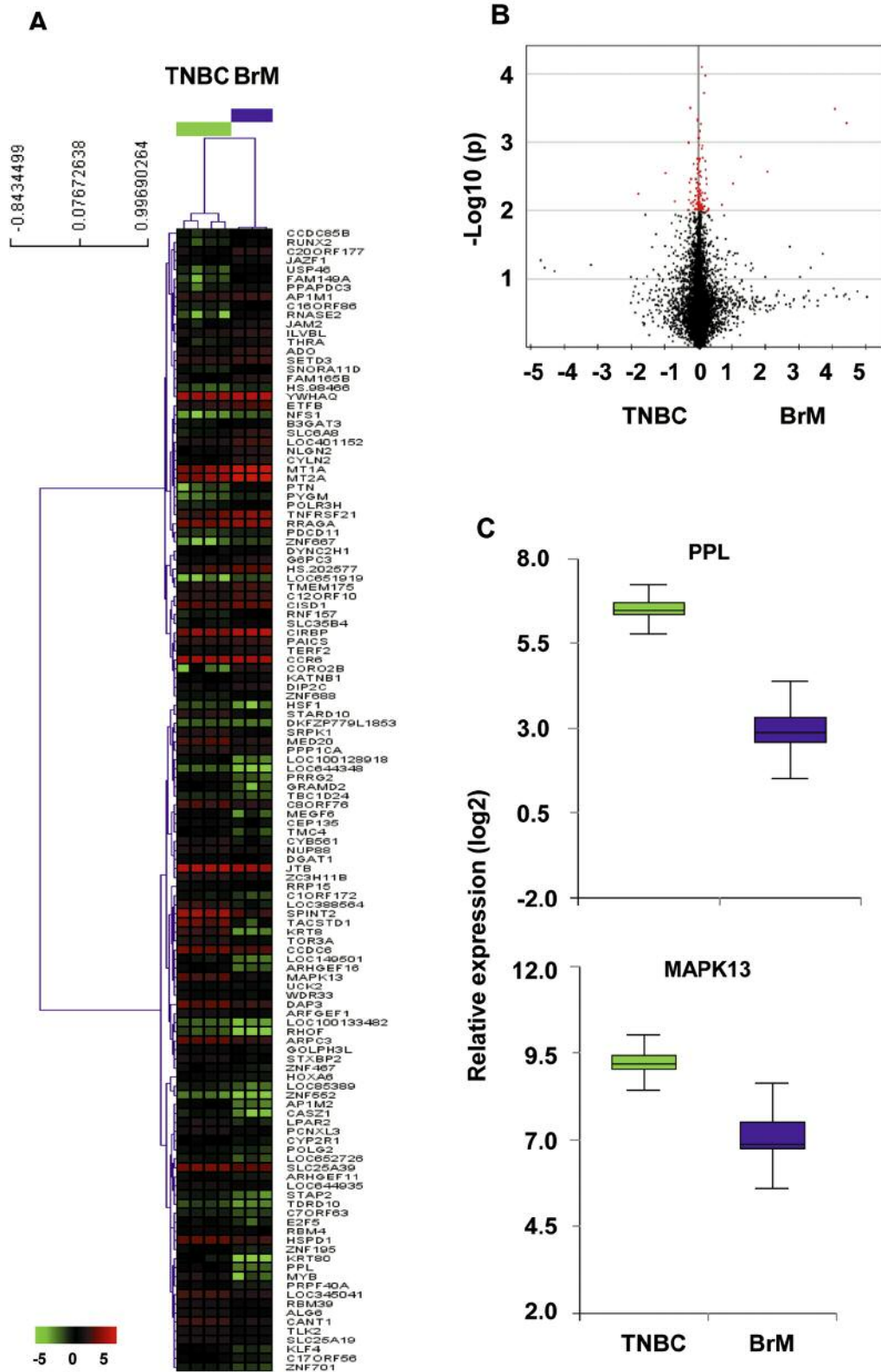


Figure 1. Different gene expression patterns in triple-negative breast cancer (TNBC) and brain-metastatic cancer (BrM). A: Heat-map shows genes differentially expressed in TNBC and BrM. B: Volcano plot presents differential expression patterns of genes in BrM and TNBC. Genes up/downregulated by 5-fold are colored in red. C: Relative expression levels of PPL (top) and MAPK13 (bottom) in TNBC and BrM.

Table I. *Genes down/up-regulated in brain-metastatic cancer (BrM) compared to triple-negative breast cancer (TNBC).*

Down/ Up-regulation	Gene	Chr	BrM	TNBC	Fold change (BrM/TNBC)	Δ Exp (BrM-TNBC)	p-Value	Full gene name
Down	<i>BAIAP2L1</i>	7	1.4±1.4	279.8±126.0	206.1	278.4	0.01	BAI1-associated protein 2-like 1
Down	<i>GRHL2</i>	8	0.5±0.0	86.8±39.1	173.5	86.3	0.01	Grainyhead-like 2 (Drosophila)
Down	<i>KRT80</i>	12	0.5±0.0	55.7±16.8	111.3	55.2	0.003	Keratin 80
Down	<i>KRT8</i>	12	4.5±1.1	466.6±137.5	104.5	462.1	0.002	Keratin 8
Down	<i>LOC644743</i>	1	3.6±4.2	277.8±104.9	77.5	274.2	0.007	KRT8P47: keratin 8 pseudogene 47
Down	<i>TJP3</i>	19	1.2±0.6	85.8±33.5	74.2	84.6	0.008	Tight junction protein 3 (zona occludens 3)
Down	<i>RAB25</i>	1	10.2±5.8	574.6±206.6	56.1	564.3	0.006	RAB25, member RAS oncogene family
Down	<i>EPCAM</i>	2	36.0±23.8	1053.1±360.4	29.2	1017.1	0.005	Epithelial cell adhesion molecule
Down	<i>CD24</i>	Y	83.7±89.7	2409.1±818.1	28.8	2325.4	0.005	CD24 molecule
Down	<i>TACSTD1</i>	2	39.2±26.1	1090.0±315.7	27.8	1050.9	0.002	Tumor-associated calcium signal transducer 1
Down	<i>MYB</i>	6	9.1±8.8	216.2±68.4	23.8	207.2	0.004	v-myb Myeloblastosis viral oncogene homolog (avian)
Down	<i>MUC1</i>	1	42.6±10.4	859.6±313.3	20.2	817.1	0.007	Mucin 1, cell surface associated
Down	<i>FAM83H</i>	8	21.4±4.0	317.3±102.3	14.8	295.9	0.005	Family with sequence similarity 83, member H
Down	<i>PPL</i>	16	8.0±2.0	95.2±16.8	12.0	87.2	0.0003	Periplakin
Down	<i>TSTD1</i>	1	9.7±4.2	114.5±45.9	11.8	104.8	0.01	Thiosulfate sulfurtransferase (rhodanese)-like domain containing 1
Down	<i>LOC388564</i>	19	38.3±14.6	435.0±105.5	11.4	396.7	0.001	Hypothetical gene supported by BC052596
Down	<i>AP1M2</i>	19	6.9±1.8	77.0±17.1	11.2	70.1	0.001	Adaptor-related protein complex 1, mu 2 subunit
Down	<i>PRRG2</i>	19	11.1±4.0	118.4±19.2	10.7	107.3	0.0002	Proline rich Gla (G-carboxyglutamic acid) 2 similar to Keratin 8
Down	<i>LOC647954</i>	5	14.2±6.2	149.1±54.7	10.5	134.9	0.009	
Down	<i>GRAMD2</i>	15	9.1±7.1	93.5±13.6	10.3	84.4	0.0002	GRAM domain containing 2
Down	<i>LOC100128918</i>	6	6.2±2.8	58.6±16.7	9.5	52.5	0.003	Hypothetical protein LOC100128918
Down	<i>ARHGEF16</i>	1	10.7±3.3	99.4±19.0	9.3	88.7	0.0005	Rho guanine exchange factor (GEF) 16
Down	<i>SPINT2</i>	19	457.2±210.6	3078.0±680.8	6.7	2620.8	0.001	Serine peptidase inhibitor, Kunitz type, 2
Down	<i>MEGF6</i>	1	16.2±16.1	107.1±19.0	6.6	90.9	0.001	Multiple EGF-like-domains 6
Down	<i>LPAR2</i>	19	32.6±14.6	215.5±58.2	6.6	183.0	0.003	Lysophosphatidic acid receptor 2
Down	<i>C11orf82</i>	11	13.1±20.8	81.3±24.5	6.2	68.3	0.01	Noxin
Down	<i>HOXC8</i>	12	29.4±43.8	166.1±53.9	5.7	136.7	0.02	Homeobox C8
Down	<i>GPATCH2</i>	1	14.4±12.5	74.9±22.2	5.2	60.5	0.009	G patch domain containing 2
Down	<i>E2F5</i>	8	24.3±15.2	115.2±28.6	4.7	90.8	0.004	E2F transcription factor 5, p130-binding
Down	<i>EDG4</i>	19	66.3±28.2	307.1±80.6	4.6	240.9	0.005	Endothelial differentiation, lysophosphatidic acid G-protein-coupled receptor, 4
Down	<i>CYB561</i>	17	52.5±34.0	236.7±56.1	4.5	184.2	0.004	Cytochrome b-561
Down	<i>LOC729964</i>	11	18.8±13.2	84.6±29.9	4.5	65.8	0.02	similar to Cks1 protein homologue
Down	<i>MAPK13</i>	6	137.0±41.3	614.2±98.9	4.5	477.2	0.0006	Mitogen-activated protein kinase 13
Down	<i>TMC4</i>	19	21.7±14.8	94.6±23.7	4.4	72.9	0.006	Transmembrane channel-like 4
Down	<i>CKS1B</i>	1	238.9±147.2	1028.5±315.0	4.3	789.5	0.01	CDC28 protein kinase regulatory subunit 1B
Down	<i>KCNN4</i>	19	28.3±7.6	120.7±44.8	4.3	92.4	0.02	Potassium intermediate/small conductance calcium-activated channel, subfamily N, member 4
Down	<i>LDLR</i>	19	131.9±97.8	540.0±154.7	4.1	408.1	0.01	Low density lipoprotein receptor
Down	<i>LOC642299</i>	1	32.0±8.2	128.6±42.0	4.0	96.5	0.01	Hypothetical protein LOC642299
Down	<i>C11orf80</i>	11	39.9±32.1	159.7±48.8	4.0	119.9	0.01	Chromosome 11 open reading frame 80
Down	<i>JUP</i>	17	77.7±7.3	306.7±113.5	3.9	229.0	0.02	Junction plakoglobin
Down	<i>NBEAL2</i>	3	32.7±10.7	113.7±32.7	3.5	81.0	0.01	Neurobeachin-like 2
Down	<i>PRPF40A</i>	2	31.3±3.3	100.7±20.0	3.2	69.5	0.002	PRP40 pre-mRNA processing factor 40 homolog A (<i>S. cerevisiae</i>)
Down	<i>CMTM8</i>	3	80.2±16.3	253.3±63.5	3.2	173.1	0.006	CKLF-like MARVEL transmembrane domain containing 8
Down	<i>OCIAD2</i>	4	141.4±48.7	446.4±140.3	3.2	305.0	0.02	OCIA domain containing 2
Down	<i>KIAA1671</i>	22	115.2±85.6	361.4±67.9	3.1	246.2	0.008	KIAA1671 protein
Up	<i>PCDH20</i>	13	79.4±47.9	0.9±0.5	87.7	78.5	0.02	Protocadherin 20
Up	<i>ZBTB16</i>	11	191.7±55.2	8.4±4.1	22.8	183.3	0.001	Zinc finger and BTB domain containing 16

Table I. *continued*

Table I. *continued*

Down/ Up-regulation	Gene	Chr	BrM	TNBC	Fold change (BrM/TNBC)	Δ Exp (BrM-TNBC)	p-Value	Full gene name
Up	<i>CORO2B</i>	15	294.4±41.6	19.8±30.9	14.8	274.6	0.0002	Coronin, actin binding protein, 2B
Up	<i>RNASE2</i>	14	117.6±13.5	8.5±8.9	13.8	109.1	0.00005	Ribonuclease, RNase A family, 2 (liver, eosinophil-derived neurotoxin)
Up	<i>PTN</i>	7	113.7±8.1	10.5±8.1	10.8	103.2	0.00001	Pleiotrophin
Up	<i>SERPINA5</i>	14	107.4±27.0	11.8±7.6	9.1	95.6	0.001	Serpin peptidase inhibitor, clade A (alpha-1 antiproteinase, antitrypsin), member 5
Up	<i>MTSS1L</i>	16	96.2±21.1	11.6±7.1	8.3	84.6	0.0006	Metastasis suppressor 1-like
Up	<i>CPT1C</i>	19	352.2±103.0	44.2±25.8	8.0	308.0	0.002	Carnitine palmitoyltransferase 1C
Up	<i>CLIP3</i>	19	2064.4±1043.6	270.8±113.0	7.6	1793.6	0.02	CAP-GLY domain containing linker protein 3
Up	<i>DACT3</i>	19	598.1±246.4	80.6±41.0	7.4	517.4	0.008	Dapper, antagonist of beta-catenin, homolog 3 (<i>Xenopus laevis</i>)
Up	<i>SEC14L2</i>	22	94.4±40.0	12.7±13.9	7.4	81.6	0.01	SEC14-like 2 (<i>S. cerevisiae</i>)
Up	<i>JAM3</i>	11	1876.4±571.2	255.8±128.8	7.3	1620.6	0.002	Junctional adhesion molecule 3
Up	<i>SIGLEC10</i>	19	349.7±122.8	49.8±54.7	7.0	299.9	0.007	Sialic acid binding Ig-like lectin 10
Up	<i>FCGBP</i>	19	900.3±256.1	131.0±61.5	6.9	769.3	0.002	Fc fragment of IgG binding protein
Up	<i>LOC402560</i>	7	78.7±34.0	11.9±9.5	6.6	66.8	0.01	Hypothetical LOC402560
Up	<i>GSTM5</i>	1	65.9±14.3	10.2±7.6	6.5	55.7	0.001	Glutathione S-transferase M5
Up	<i>VSIG4</i>	X	1226.2±267.4	190.1±200.7	6.4	1036.1	0.002	V-set and Immunoglobulin domain containing 4
Up	<i>MTE</i>	16	563.6±141.2	89.2±37.6	6.3	474.4	0.001	MT1IP: Metallothionein 1I, pseudogene
Up	<i>SFXN5</i>	2	426.0±60.0	68.9±31.2	6.2	357.1	0.0001	Sideroflexin 5
Up	<i>TSPAN5</i>	4	186.7±43.0	30.3±11.6	6.2	156.4	0.0008	Tetraspanin 5
Up	<i>PPAPDC3</i>	9	163.9±17.7	26.8±14.2	6.1	137.0	0.00009	Phosphatidic acid phosphatase type 2 domain containing 3
Up	<i>APLN</i>	X	215.0±71.5	35.4±19.9	6.1	179.6	0.004	Apelin
Up	<i>PTH1R</i>	3	117.3±39.2	19.9±5.1	5.9	97.3	0.004	Parathyroid hormone 1 receptor
Up	<i>FAT3</i>	11	70.0±32.9	12.2±3.7	5.8	57.9	0.02	FAT tumor suppressor homolog 3
Up	<i>SLC6A8</i>	X	368.9±75.3	65.5±55.7	5.6	303.4	0.002	Solute carrier family 6 (neurotransmitter transporter, creatine), member 8
Up	<i>CPE</i>	4	1497.2±427.6	267.5±64.1	5.6	1229.7	0.002	Carboxypeptidase E
Up	<i>C2orf32</i>	2	229.5±84.6	41.5±34.3	5.5	188.0	0.009	CNRIP1: cannabinoid receptor interacting protein 1
Up	<i>CPS1</i>	2	148.8±69.5	27.4±14.6	5.4	121.4	0.02	Carbamoyl-phosphate synthetase 1, mitochondrial
Up	<i>FAM149A</i>	4	68.3±6.7	12.7±7.8	5.4	55.7	0.0002	Family with sequence similarity 149, member A
Up	<i>SPRY2</i>	13	511.2±160.6	95.6±54.9	5.3	415.6	0.004	Sprouty homolog 2 (<i>Drosophila</i>)
Up	<i>CLIP2</i>	7	216.9±55.1	41.0±15.4	5.3	175.9	0.002	CAP-GLY domain containing linker protein 2
Up	<i>MT1E</i>	16	1852.4±519.3	350.7±157.6	5.3	1501.7	0.002	Metallothionein 1E (functional)
Up	<i>DKK3</i>	11	1424.5±618.3	303.6±128.4	4.7	1121.0	0.01	Dickkopf homolog 3 (<i>Xenopus laevis</i>)
Up	<i>USP46</i>	4	79.7±14.8	17.1±10.8	4.7	62.6	0.001	Ubiquitin specific peptidase 46
Up	<i>CYLN2</i>	7	338.9±19.8	76.2±24.9	4.4	262.7	0.00002	Cytoplasmic linker 2
Up	<i>C20orf127</i>	20	243.7±57.8	55.0±23.7	4.4	188.7	0.002	MT1P3: Metallothionein 1 pseudogene 3
Up	<i>FAM38B</i>	18	285.8±106.2	64.9±39.3	4.4	220.8	0.01	Family with sequence similarity 38, member B
Up	<i>SLC6A10P</i>	16	526.6±96.6	119.6±145.1	4.4	406.9	0.009	Solute carrier family 6 (neurotransmitter transporter, creatine), member 10 (pseudogene)
Up	<i>PTPN13</i>	4	129.9±48.5	30.0±21.7	4.3	99.9	0.01	Protein tyrosine phosphatase, non-receptor type 13 (APO-1/CD95 (Fas)-associated phosphatase)
Up	<i>ZHX3</i>	20	359.0±136.6	83.6±43.6	4.3	275.4	0.01	Zinc fingers and homeoboxes 3
Up	<i>ALDH6A1</i>	14	493.0±199.4	114.8±40.9	4.3	378.2	0.01	Aldehyde dehydrogenase 6 family, member A1
Up	<i>THRA</i>	17	166.4±28.0	39.0±18.8	4.3	127.4	0.0008	Thyroid hormone receptor, alpha (erythroblastic leukemia viral (v-erb-a) oncogene homolog, avian)

Table I. *continued*

Table I. *continued*

Down/ Up-regulation	Gene	Chr	BrM	TNBC	Fold change (BrM/TNBC)	Δ Exp (BrM-TNBC)	p-Value	Full gene name
Up	<i>SMARCD3</i>	7	124.5±50.1	29.6±16.2	4.2	94.9	0.01	SWI/SNF related, matrix associated, actin dependent regulator of chromatin, subfamily d, member 3
Up	<i>RNASE1</i>	14	2600.7±851.2	627.4±271.0	4.1	1973.3	0.007	Ribonuclease, RNase A family, 1 (pancreatic)
Up	<i>MT2A</i>	16	8298.1±236.3	2021.9±722.6	4.1	6276.2	0.00003	Metallothionein 2A
Up	<i>SPP1</i>	4	6986.8±1726.8	1718.9±930.4	4.1	5267.9	0.003	Secreted phosphoprotein 1
Up	<i>HABP4</i>	9	311.0±107.0	78.4±14.3	4.0	232.6	0.007	Hyaluronan binding protein 4
Up	<i>MT1A</i>	16	7773.0±460.0	1984.8±839.8	3.9	5788.2	0.0001	Metallothionein 1A
Up	<i>LOC441019</i>	4	116.5±37.7	30.0±11.5	3.9	86.6	0.007	Hypothetical LOC441019
Up	<i>MT1X</i>	16	5199.0±1543.7	1338.6±980.5	3.9	3860.5	0.009	Metallothionein 1X
Up	<i>CD163</i>	12	1938.9±614.8	503.0±473.4	3.9	1435.9	0.02	CD163 molecule
Up	<i>GPR177</i>	1	335.2±119.5	87.1±32.9	3.8	248.1	0.01	G protein-coupled receptor 177
Up	<i>PTPRH</i>	19	81.8±27.6	21.4±14.6	3.8	60.4	0.01	Protein tyrosine phosphatase, receptor type, H
Up	<i>SPARCL1</i>	4	3799.8±1477.9	994.3±582.9	3.8	2805.6	0.02	SPARC-like 1 (mast9, hevjin)
Up	<i>CNRIP1</i>	2	265.6±72.7	69.8±51.7	3.8	195.8	0.008	Cannabinoid receptor interacting protein 1
Up	<i>SLC2A5</i>	1	917.8±316.0	250.7±123.0	3.7	667.2	0.01	Solute carrier family 2 (facilitated glucose/fructose transporter), member 5
Up	<i>KLF9</i>	9	1494.4±477.4	409.8±250.2	3.6	1084.6	0.01	Kruppel-like factor 9
Up	<i>FAM108A3</i>	1	134.4±45.3	37.0±12.9	3.6	97.4	0.008	Family with sequence similarity 108, member A3
Up	<i>CCDC106</i>	19	363.0±64.8	101.5±37.0	3.6	261.5	0.001	Coiled-coil domain containing 106
Up	<i>MERTK</i>	2	350.0±119.9	98.9±60.0	3.5	251.0	0.01	c-Met proto-oncogene tyrosine kinase
Up	<i>DCTN1</i>	2	618.7±146.3	182.5±61.0	3.4	436.3	0.003	Dynactin 1 (p150, glued homolog, Drosophila)
Up	<i>RNF144A</i>	2	460.3±78.7	137.1±28.2	3.4	323.2	0.0006	Ring finger protein 144A
Up	<i>F3</i>	1	114.2±32.8	34.0±14.4	3.4	80.2	0.007	Coagulation factor III
Up	<i>TCEA2</i>	20	247.0±74.6	74.7±33.2	3.3	172.3	0.009	Transcription elongation factor A (SII), 2
Up	<i>RNF144</i>	2	721.5±144.8	218.2±19.9	3.3	503.3	0.0009	Ring finger protein 144
Up	<i>DDIT4L</i>	4	208.5±49.8	64.5±37.8	3.2	144.0	0.007	DNA-damage-inducible transcript 4-like
Up	<i>FPR1</i>	19	292.9±62.9	90.7±48.8	3.2	202.2	0.005	Formyl peptide receptor 1
Up	<i>TNFRSF21</i>	6	2094.5±308.2	662.6±316.4	3.2	1431.9	0.002	Tumor necrosis factor receptor superfamily, member 21
Up	<i>THNSL2</i>	2	95.3±32.9	30.7±12.9	3.1	64.6	0.01	Threonine synthase-like 2
Up	<i>ARRDC4</i>	15	112.5±34.4	36.2±17.7	3.1	76.3	0.01	Arrestin domain containing 4
Up	<i>LOC644869</i>	5	87.0±14.5	28.2±21.4	3.1	58.8	0.01	Hypothetical protein LOC644869
Up	<i>LOC100128252</i>	19	231.1±14.0	75.0±69.6	3.1	156.1	0.01	similar to MGC9913 protein
Up	<i>WDR22</i>	14	406.0±157.8	132.0±11.5	3.1	273.9	0.02	WD repeat domain 22
Up	<i>JAM2</i>	21	215.8±39.7	71.3±40.4	3.0	144.5	0.005	Junctional adhesion molecule 2

levels of PPL and MAPK13 were higher in MDA-MB-231, Hs578T, HCC-70, HCC-38 and HCC-1395 than in GBL-60 (Figure 2B).

PPL and MAPK13 facilitate TNBC cell growth. Thus, we further examined whether silencing of either PPL or MAPK13 affects the growth of TNBC cells. When expression of either PPL or MAPK13 in MDA-MB-231, Hs578T and HCC-70 cells were knocked-down with appropriate siRNAs, the growth rates of these cells were higher than those of cells where control siRNA was

transfected (Figure 3A and C). In detail, whereas the doubling time of MDA-MB-231 cells was 41.81 h, in cells where either *PPL* or *MAPK13* was silenced, the doubling time became 34.76 and 32.58 h, respectively. The doubling time of Hs578T cells was 38.94 h, while *PPL* and *MAPK13* silencing led to times of 33.34 and 33 h, respectively. In the case of HCC-70 cells, control, PPL or MAPK13 siRNA led to 29.46, 27.73 and 27.05 h, respectively, for the doubling time. Conversely, when overexpression of PPL or MAPK13 was induced in GBL-60 cells, the doubling time (31.98 h) was extended to 40.16 h with PPL and 42.05 h with

Table II. *Ontology of genes differentially expressed in brain-metastatic cancer (BrM) compared to triple-negative breast cancer (TNBC).*

Group	Gene ontology category	Genes	Number of genes in category			Ratio of enrichment	<i>p</i> -Value	Adjusted <i>p</i> -Value	
			Reference	Observed	Expected				
Down-regulation	Cellular component	Apical junction complex (GO:0043296)	<i>PPL, TJP3, JUP</i>	89	3	0.18	16.67	0.0007	0.01
		Apicolateral plasma membrane (GO:0016327)	<i>PPL, TJP3, JUP</i>	92	3	0.19	16.13	0.0008	0.01
		Desmosome (GO:0030057)	<i>PPL, JUP</i>	19	2	0.04	52.07	0.0007	0.01
		Plasma membrane part (GO:0044459)	<i>EPCAM, MUC1, CD24, LPAR2, TJP3, JUP, KCNN4, LDLR, CYB561, PPL, PRRG2</i>	1752	11	3.54	3.11	0.0004	0.01
Up-regulation	Molecular function	Cadmium ion binding (GO:0046870)	<i>MTIX, MT1A, MTIE</i>	9	3	0.03	92.58	3.6E-06	0.0003
		Protease binding (GO:0002020)	<i>SERPINA5, F3</i>	18	2	0.06	30.86	0.002	0.03
		Pancreatic ribonuclease activity (GO:0004522)	<i>RNASE2, RNASE1</i>	14	2	0.05	39.68	0.001	0.03
		Endoribonuclease activity, producing 3'-phospho-monoesters (GO:0016892)	<i>RNASE2, RNASE1</i>	17	2	0.06	32.67	0.002	0.03
		Copper ion binding (GO:0005507)	<i>MTIX, MT1A, MTIE</i>	59	3	0.21	14.12	0.001	0.03
		Endonuclease activity, active with either ribo- or deoxyribonucleic acids and producing 3'-phospho-monoesters (GO:0016894)	<i>RNASE2, RNASE1</i>	22	2	0.08	25.25	0.003	0.04

Table III. *Pathway analysis of genes differentially regulated in brain-metastatic cancer (BrM) compared to triple-negative breast cancer (TNBC).*

Rank	Pathway name	Genes	Impact factor	Genes in pathway (n)	Input genes in pathway (n)	Pathway genes on chip (n)	Input genes in pathway (%)	Pathway genes in input (%)	<i>p</i> -Value	Corrected <i>p</i> -Value	Gamma <i>p</i> -value	Corrected gamma <i>p</i> -value
1	Epithelial cell signaling in <i>Helicobacter pylori</i> infection	<i>JAM2, JAM3, MAPK13</i>	8.3	68	3	68	2.7	4.4	0.003	0.003	0.002	0.002
2	Tight junction	<i>JAM2, JAM3, TJP3</i>	8.0	135	3	131	2.7	2.2	0.021	0.021	0.003	0.003
3	Cell adhesion molecules (CAMs)	<i>JAM2, JAM3</i>	7.6	134	2	129	1.8	1.5	0.113	0.113	0.004	0.004
4	Complement and coagulation cascades	<i>F3, 5, SERPINA</i>	6.0	69	2	68	1.8	2.9	0.037	0.037	0.017	0.017
5	Leukocyte transendothelial migration	<i>JAM2, JAM3, MAPK13</i>	5.2	119	3	115	2.7	2.5	0.015	0.015	0.034	0.034
6	Acute myeloid leukemia	<i>JUP, JBTB16</i>	4.9	59	2	57	1.8	3.4	0.027	0.027	0.045	0.045

MAPK13, respectively (Figure 3B and C). Therefore, our data indicate that altered gene expression of either *PPL* or *MAPK13* may affect TNBC cell growth rate.

To examine whether *PPL* and *MAPK13* affect metastatic growth ability, we performed anchorage-independent growth assays. Silencing of either *PPL* or *MAPK13* increased colony numbers in TNBC cell lines MDA-MB-231, Hs578T and HCC-70, whereas overexpression of either *PPL* or *MAPK13* reduced colony formation in GBL-60 cells (Figure 3D).

PPL and *MAPK13* repress TNBC cell motility. We next examined whether silencing of *PPL* and *MAPK13* affects cell migration ability. In MDA-MB-231, Hs578T and HCC-70 cells, silencing of either *PPL* or *MAPK13* reduced cell migration rates (Figure 4A). We also found that silencing of either *PPL* or *MAPK13* retarded invasiveness of MDA-MB-231, Hs578T and HCC-70 cells (Figure 4B). However, overexpression of either *PPL* or *MAPK13* in GBL-60 cells facilitated cell migration and invasion (Figure 4A and 4B). Thus, our data further suggest that expression levels of *PPL* and *MAPK13* may determine TNBC cell motility.

Discussion

Metastasis of TNBC to the brain occurs frequently, resulting in a high risk of death (5-8). While genes associated with distant metastases of breast cancer have been investigated, genes involved in metastasis of TNBC to the brain are yet to be reported (6, 9, 14, 22). Our study demonstrates that 119 genes were differentially expressed between TNBC and BrM. Gene ontology and pathway analyses showed that genes involved in cell-to-cell interaction were affected in BrM. These data indicate that TNBC cells have altered expression levels of genes involved in cell-to-cell interaction. From the analyses, we found that expression patterns of two genes, *PPL* and *MAPK13*, were significantly different between BrM and TNBC. Moreover, altered expression of either *PPL* or *MAPK13* affected TNBC growth and motility, *in vitro*.

PPL is crucial for maintaining epithelial cell barriers in normal physiology (24-26). Recent research revealed that cyclin A2-induced up-regulation of *PPL* is associated with aggressive behavior as well as cisplatin resistance of endometrial cancer cells (27). Likewise, *PPL* silencing reduced migration and attachment of pharyngeal squamous cancer cells (28). *PPL* down-regulation was correlated with the progression of esophageal squamous cell carcinoma (29, 30). In our study, *PPL* silencing reduced TNBC cell migration and invasion, while increasing cell growth even in soft agar. Thus, reduced expression of *PPL* in BrM suggests that down-regulation of *PPL* is important for TNBC cell growth in the brain.

MAPK13 was found to promote cholangiocarcinoma cell invasiveness (31), while *MAPK13* DNA was found to be

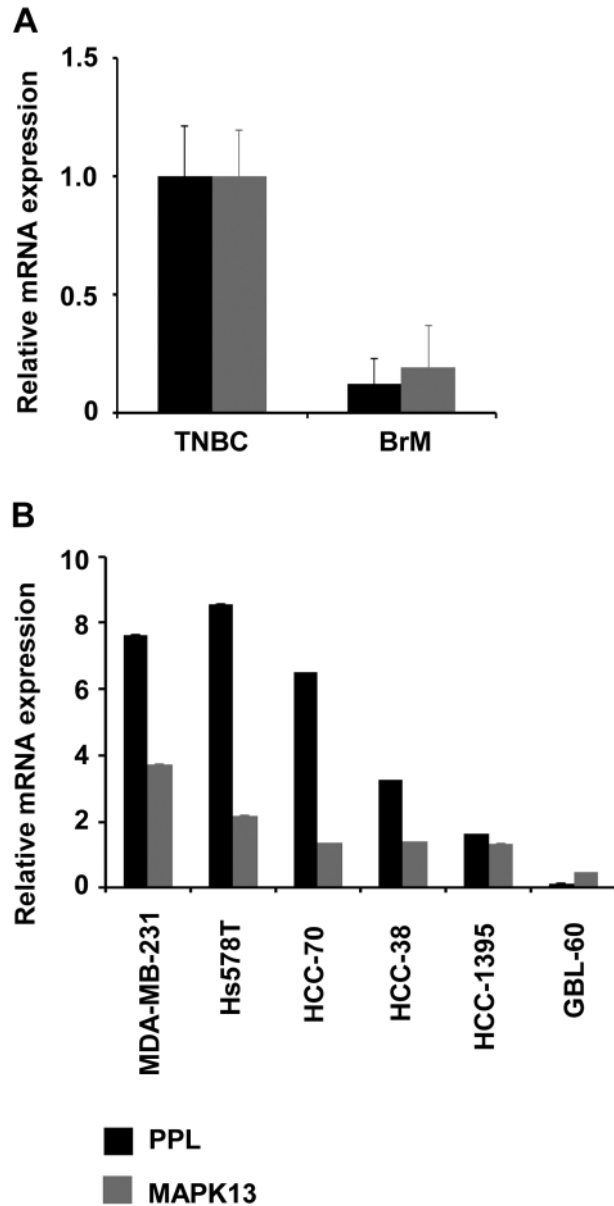


Figure 2. Expression of periplakin (*PPL*) and mitogen-activated protein kinase 13 (*MAPK13*). A: mRNA levels of *PPL* and *MAPK13* in brain-metastatic cancer (BrM) and triple-negative breast cancer (TNBC). Glyceraldehyde 3-phosphoate dehydrogenase (*GAPDH*) mRNA was measured as an internal control. Relative values were measured by normalizing 2^{-ddCT} (BrM vs. TNBC). B: mRNA levels of *PPL* and *MAPK13* in TNBC cell lines (MDA-MB-231, Hs578T, HCC-70, HCC-38 and HCC-1395) and BrM cells (GBL-60).

methyated in malignant pleural mesothelioma (32). In the highly metastatic TNBC MDA-MB-231 cell line, tissue inhibitor of metallo-proteinase 1 (TIMP-1) overexpression down-regulated *MAPK13* expression and led to an inhibition of cell motility (33). Consistent with this, our study also

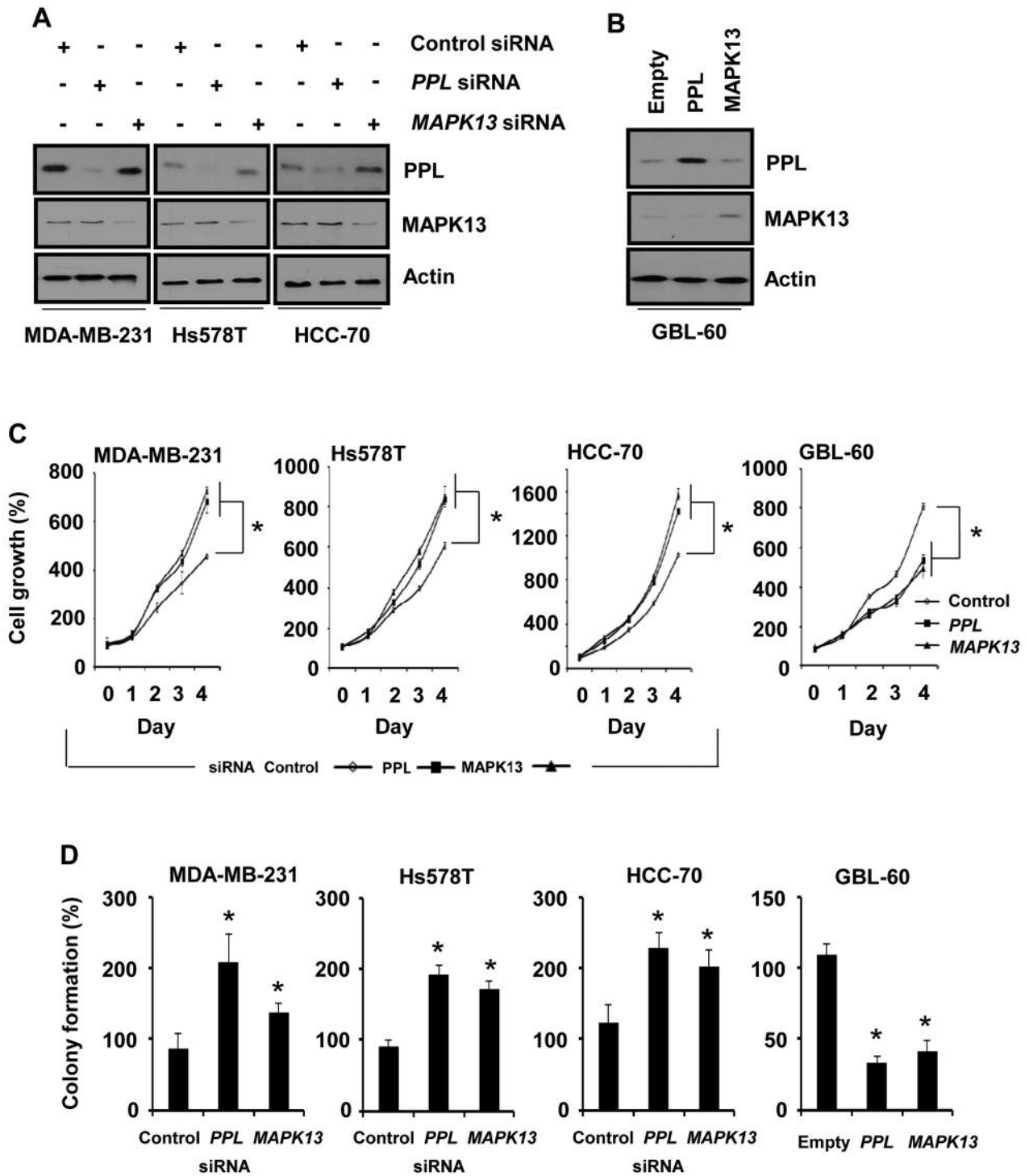


Figure 3. Silencing of either periplakin (PPL) or mitogen-activated protein kinase 13 (MAPK13) facilitates triple-negative breast cancer (TNBC) cell growth. A: Expression of PPL and MAPK13 in different TNBC cells (MDA-MB-231, Hs578T and HCC-70) silenced with control, PPL or MAPK13 siRNA. B: Overexpression of PPL and MAPK13 in GBL-60 cells. Appropriate antibodies were used to detect PPL and MAPK13. Actin was used as an internal control. C: Cell growth rates of MDA-MB-231, Hs578T, HCC-70 and GBL-60 cells, where expression of either PPL or MAPK13 was altered. Cell numbers were counted for four days. D: Anchorage-independent cell growth. TNBC and BrM cells where expression of either PPL or MAPK13 was altered were cultured in soft agar. Fifteen days after incubation, plates were stained with crystal violet and colonies were counted. *p-Values less than 0.05 were considered significantly different from the controls.

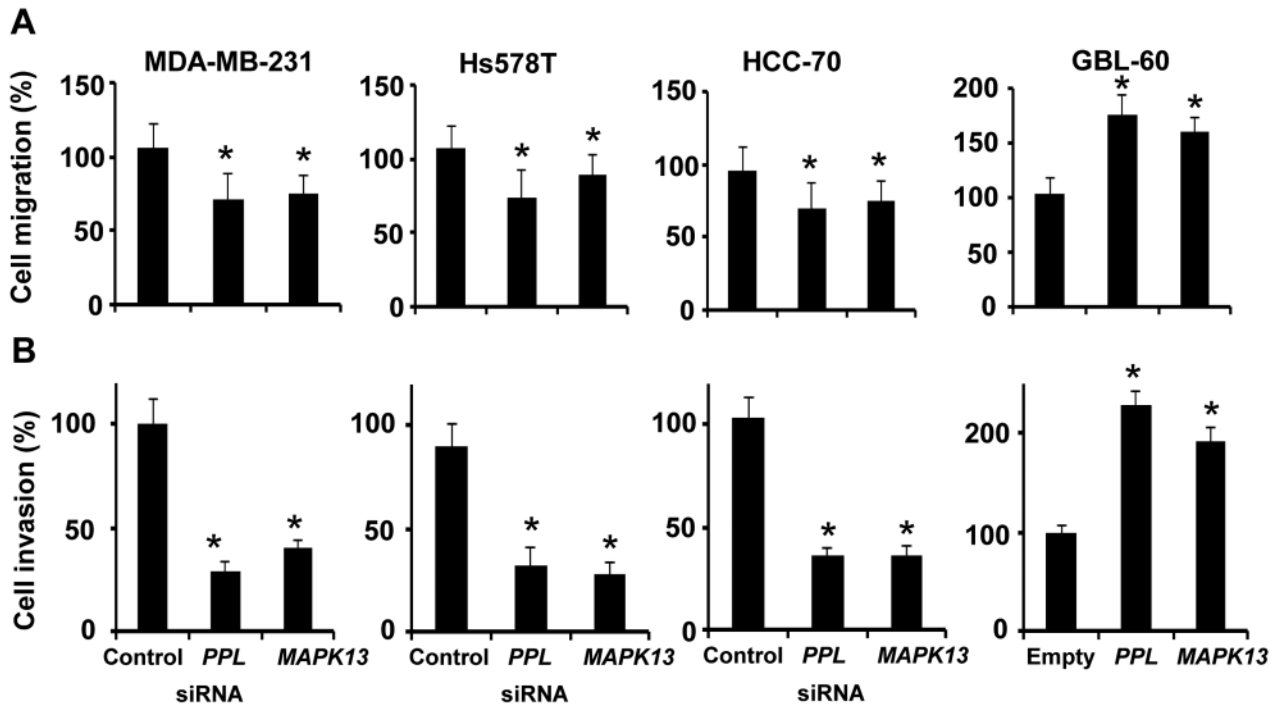


Figure 4. Periplakin (PPL) and mitogen-activated protein kinase 13 (MAPK13) regulate cell motility. A: Migration rates of triple-negative breast cancer (TNBC) and brain-metastatic cancer (BrM) cells where expression of either PPL or MAPK13 was altered. Cell culture plates were scratched and then cells were further cultured for one day. Migrated cells were counted after randomly choosing four fields in scratched regions. B: Invasiveness of TNBC and BrM, where expression of either PPL or MAPK13 was altered. Cells were cultured on top chambers filled with 1% serum and allowed to invade toward the bottom chambers filled with 10% serum. Invaded cells were stained with crystal violet and counted. *p-Values less than 0.05 were considered significantly different from controls.

showed that *MAPK13* silencing reduced both migration and invasion of TNBC cells. However, *MAPK13* silencing induced cell growth even in soft agar, which was similar to the effect of *PPL* silencing on cell growth. Thus, down-regulation of *PPL* and *MAPK13* in BrM indicates that TNBC cells require cell growth ability rather than motility in the brain. Cellular phenomena resulting from the effect of *PPL* and *MAPK13* are similar to those resulting from the activation of metastasis suppressor genes (34-39). Thus, our data are consistent with the notion that metastasis suppressor genes are down-regulated in metastatic cancer. However, it is yet unclear whether *PPL* and *MAPK13* play the role of metastasis suppressors in TNBC.

Overall, TNBC cells may alter gene expression patterns for the growth in the brain. However, it is unclear whether expression patterns of particular genes drive BrM, regardless of breast cancer subtype. Thus, our ongoing studies will strive to identify common gene sets driving BrM. In addition, BrM of TNBC is associated with poor outcomes (10, 16-19, 21, 40). Thus, identifying gene signatures driving TNBC metastasis to the brain will provide knowledge for understanding the nature of BrM, improving diagnostic and therapeutic approaches.

Acknowledgements

This study was supported by a grant from Korean Medicine R&D Project of the Ministry of Health and Welfare (B110043).

References

- Minn AJ, Gupta GP, Siegel PM, Bos PD, Shu W, Giri DD *et al*: Genes that mediate breast cancer metastasis to lung. *Nature* 436: 518-524, 2005.
- Masuda S: Breast cancer pathology: the impact of molecular taxonomy on morphological taxonomy. *Pathol Int* 62: 295-302, 2012.
- Wilhelm I, Molnar J, Fazakas C, Hasko J and Krizbai IA: Role of the blood-brain barrier in the formation of brain metastases. *Int J Mol Sci* 14: 1383-1411, 2013.
- Lim B, Cream LV and Harvey HA: Update on clinical trials: genetic targets in breast cancer. *Adv Exp Med Biol* 779: 35-54, 2013.
- Mao Y, Keller ET, Garfield DH, Shen K and Wang J: Stromal cells in tumor microenvironment and breast cancer. *Cancer Metastasis Rev*, 2012.
- Scully OJ, Bay BH, Yip G and Yu Y: Breast cancer metastasis. *Cancer Genomics & Proteomics* 9: 311-320, 2012.
- Burstein HJ, Polyak K, Wong JS, Lester SC and Kaelin CM: Ductal carcinoma *in situ* of the breast. *N Eng J Med* 350: 1430-1441, 2004.

- 8 Sotiriou C and Puzstai L: Gene-expression signatures in breast cancer. *N Eng J Med* 360: 790-800, 2009.
- 9 Foulkes WD, Smith IE and Reis-Filho JS: Triple-negative breast cancer. *N Eng J Med* 363: 1938-1948, 2010.
- 10 Penault-Llorca F and Viale G: Pathological and molecular diagnosis of triple-negative breast cancer: a clinical perspective. *Annals of oncology: official journal of the European Society for Medical Oncology/ESMO* 23(Suppl 6): vi19-22, 2012.
- 11 Andre F and Zielinski CC: Optimal strategies for the treatment of metastatic triple-negative breast cancer with currently approved agents. *Ann Oncol: official journal of the European Society for Medical Oncology/ESMO* 23(Suppl 6): vi46-51, 2012.
- 12 Dogan BE and Turnbull LW: Imaging of triple-negative breast cancer. *Ann Oncol: official journal of the European Society for Medical Oncology/ESMO* 23(Suppl 6): vi23-29, 2012.
- 13 Freedman RA, Anders CK: Treatment of Breast Cancer Brain Metastases. *Curr Breast Cancer Rep* 4: 1-9, 2012.
- 14 Espinosa E, Vara JA, Navarro IS, Gamez-Pozo A, Pinto A, Zamora P *et al*: Gene profiling in breast cancer: time to move forward. *Cancer Treat Rev* 37: 416-421, 2011.
- 15 de Ruijter TC, Veeck J, de Hoon JP, van Engeland M and Tjan-Heijnen VC: Characteristics of triple-negative breast cancer. *J Cancer Res Clin Oncol* 137: 183-192, 2011.
- 16 Arslan UY, Oksuzoglu B, Aksoy S, Harputluoglu H, Turker I, Ozisik Y *et al*: Breast cancer subtypes and outcomes of central nervous system metastases. *Breast* 20: 562-567, 2011.
- 17 Hines SL, Vallow LA, Tan WW, McNeil RB, Perez EA, Jain A. Clinical outcomes after a diagnosis of brain metastases in patients with estrogen- and/or human epidermal growth factor receptor 2-positive versus triple-negative breast cancer. *Ann Oncol: official journal of the European Society for Medical Oncology/ESMO* 19: 1561-155, 2008.
- 18 Lin NU, Claus E, Sohl J, Razzak AR, Arnaout A and Winer EP: Sites of distant recurrence and clinical outcomes in patients with metastatic triple-negative breast cancer: high incidence of central nervous system metastases. *Cancer* 113: 2638-2645, 2008.
- 19 Kwon HC, Oh SY, Kim SH, Lee S, Kwon KA, Choi YJ *et al*: Clinical outcomes and breast cancer subtypes in patients with brain metastases. *Onkologie* 33: 146-152, 2010.
- 20 Gupta GP, Minn AJ, Kang Y, Siegel PM, Serganova I, Cordon-Cardo C *et al*: Identifying site-specific metastasis genes and functions. *Cold Spring Harb Symp Quant Biol* 70: 149-158, 2005.
- 21 Tseng LM, Hsu NC, Chen SC, Lu YS, Lin CH, Chang DY *et al*: Distant metastasis in triple-negative breast cancer. *Neoplasma* 60: 290-294, 2013.
- 22 Bos PD, Zhang XH, Nadal C, Shu W, Gomis RR, Nguyen DX *et al*: Genes that mediate breast cancer metastasis to the brain. *Nature* 459: 1005-1009, 2009.
- 23 Kang Y, Siegel PM, Shu W, Drobnjak M, Kakonen SM, Cordon-Cardo C *et al*: A multigenic program mediating breast cancer metastasis to bone. *Cancer Cell* 3: 537-549, 2003.
- 24 Sevilla LM, Nachat R, Groot KR, Klement JF, Uitto J, Djian P *et al*: Mice deficient in involucrin, envoplakin, and periplakin have a defective epidermal barrier. *J Cell Biol* 179: 1599-1612, 2007.
- 25 Karashima T, Watt FM: Interaction of periplakin and envoplakin with intermediate filaments. *J Cell Sci* 115: 5027-5037, 2002.
- 26 Ruhrberg C, Hajibagheri MA, Parry DA, Watt FM: Periplakin, a novel component of cornified envelopes and desmosomes that belongs to the plakin family and forms complexes with envoplakin. *J Cell Biol* 139: 1835-1849, 1997.
- 27 Suzuki A, Horiuchi A, Ashida T, Miyamoto T, Kashima H, Nikaido T *et al*: Cyclin A2 confers cisplatin resistance to endometrial carcinoma cells *via* up-regulation of an Akt-binding protein, periplakin. *J Cell Mol Med* 14: 2305-2317, 2010.
- 28 Tonoike Y, Matsushita K, Tomonaga T, Katada K, Tanaka N, Shimada H *et al*: Adhesion molecule periplakin is involved in cellular movement and attachment in pharyngeal squamous cancer cells. *BMC Cell Biol* 12: 41, 2011.
- 29 Nishimori T, Tomonaga T, Matsushita K, Oh-Ishi M, Kodera Y, Maeda T *et al*: Proteomic analysis of primary esophageal squamous cell carcinoma reveals down-regulation of a cell adhesion protein, periplakin. *Proteomics* 6: 1011-1018, 2006.
- 30 Hatakeyama H, Kondo T, Fujii K, Nakanishi Y, Kato H, Fukuda S *et al*: Protein clusters associated with carcinogenesis, histological differentiation and nodal metastasis in esophageal cancer. *Proteomics* 6: 6300-6316, 2006.
- 31 Tan FL, Ooi A, Huang D, Wong JC, Qian CN, Chao C *et al*: p38delta/MAPK13 as a diagnostic marker for cholangiocarcinoma and its involvement in cell motility and invasion. *Int J Cancer* 126: 2353-2361, 2010.
- 32 Goto Y, Shinjo K, Kondo Y, Shen L, Toyota M, Suzuki H *et al*: Epigenetic profiles distinguish malignant pleural mesothelioma from lung adenocarcinoma. *Cancer Res* 69: 9073-9082, 2009.
- 33 Bigelow RL, Williams BJ, Carroll JL, Daves LK and Cardelli JA: TIMP-1 overexpression promotes tumorigenesis of MDA-MB-231 breast cancer cells and alters expression of a subset of cancer promoting genes *in vivo* distinct from those observed *in vitro*. *Breast Cancer Res Treat* 117: 31-44, 2009.
- 34 Ohtaki T, Shintani Y, Honda S, Matsumoto H, Hori A, Kanehashi K *et al*: Metastasis suppressor gene KiSS-1 encodes peptide ligand of a G-protein-coupled receptor. *Nature* 411: 613-617, 2001.
- 35 Otsuki Y, Tanaka M, Yoshii S, Kawazoe N, Nakaya K and Sugimura H: Tumor metastasis suppressor nm23H1 regulates Rac1 GTPase by interaction with Tiam1. *Proc Natl Acad Sci USA* 98: 4385-4390, 2001.
- 36 Gildea JJ, Seraj MJ, Oxford G, Harding MA, Hampton GM, Moskaluk CA *et al*: RhoGDI2 is an invasion and metastasis suppressor gene in human cancer. *Cancer Res* 62: 6418-6423, 2002.
- 37 Wyszomierski SL and Yu D: A knotty turnabout?: Akt1 as a metastasis suppressor. *Cancer Cell* 8: 437-439, 2005.
- 38 Horak CE, Lee JH, Marshall JC, Shreeve SM and Steeg PS: The role of metastasis suppressor genes in metastatic dormancy. *Apmis* 116: 586-601, 2008.
- 39 Taylor J, Hickson J, Lotan T, Yamada DS and Rinker-Schaefter C: Using metastasis suppressor proteins to dissect interactions among cancer cells and their microenvironment. *Cancer Metastasis Rev* 27: 67-73, 2008.
- 40 Xu Z, Schlesinger D, Toulmin S, Rich T and Sheehan J: Impact of triple-negative phenotype on prognosis of patients with breast cancer brain metastases. *Int J Radiat Oncol Biol Phys* 84: 612-618, 2012.

Received August 25, 2013
Revised October 24, 2013
Accepted October 25, 2013